

UDC 544.33; 544.34

SOME ASPECTS OF THE THEORY AND PRACTICE OF CORROSION AND THERMAL DESTRUCTION OF METAL MATERIALS AND OF METAL COATINGS

Platonova E.S.¹, Yurov V.M.², Eremin E.N.³, Buchinskas V.⁴, Guchenko S.A.²,
Laurynas V.Ch²

¹Karaganda State Technical University, Karaganda, Kazakhstan, danilina1969@list.ru

²Karaganda State University named after E.A Buketov, Karaganda, Kazakhstan, exciton@list.ru

³Omsk State Technical University, Omsk, Russia, weld_techn@mail.ru

⁴Vilnyusky Technical University named after Gediminas, Vilnius, Lithuania, Vytautas.Bucinskas@vgtu.lt

On the basis of the statistical approach to the formation of corrosion spots obtained an expression that shows the logarithmic dependence of the corrosion spot area of "defects" of the metal surface or coating. On the basis of a thermodynamic model obtained relationship between corrosion rate, the surface tension of a metal surface and their melting point. A method for determining the thermal stress in the coating on the basis of experimental values of microhardness, measured along and across the sample. On the basis of thermodynamic model derived relationship between the heat resistance of coatings and surface energy. A formula that is suitable for qualitative analysis and forecasting of metal fracture rate and coatings deformation and thermal influences.

Keywords: corrosion, thermal stability, metal, metal coating, a statistical model, thermodynamic model, microhardness

Introduction

Issues of metal corrosion devoted a huge amount of work, of which only work note [1-7], where an extensive bibliography. Despite this, in the field of corrosion theory continues to grow with the growth of various types of structural metallic materials used in various areas of industrial production.

In the most general case, corrosion of the metal can be present as the nucleation and growth of the new phase (oxidized metal). A critical new phase nuclei are formed sequentially in a series of random acts of attachment and detachment of atoms (molecules) from each other. Therefore, nucleation - random process in time and space. It determines the probabilistic nature of the parameters that describe the kinetics of formation of nuclei in the process of corrosion, or crystal growth [1]. A quantitative description of random process is given by its distribution function satisfies the kinetic equation. In general, the kinetic equation is a complex integral-differential equation, which cannot be solved. However, when viewed as a Markov random process, the kinetic equation becomes a differential, which has a simple form [2].

In the particular case of a Poisson process, birth and death with a finite number of states, a system of differential equations [8, 9]:

$$\begin{cases} dp_0/dt = -\lambda_0 p_0 \\ \dots \\ dp_k/dt = \lambda_{k-1} p_{k-1} - (\mu_k + \lambda_k) p_k + \mu_{k+1} p_{k+1} \\ \dots \\ dp_n/dt = \lambda_{n-1} p_{n-1} \end{cases} \quad (1)$$

Here λ_0 – is the likelihood of transition from state E_0 to E_1 , etc.; μ_1 – is the probability of transition from the state E_1 to E_0 , etc.

Therefore, it is possible to make a numerical estimate based on the actual situation of the system 1 and equation (5):

$$\ln N_0 - \ln Q_0 = N_0 \ln(\pi n_0) + 2N_0 \ln r - \pi N_0 n_0 r^2.$$

An assessment shows that the first term on the left side of the equation and the first two terms of the right - are negligible. The result:

$$N_0 = \frac{\ln Q_0}{\pi n_0 r^2}. \quad (7)$$

Given that $\pi r^2 = S$ - the area of corrosion spots and $n_0 N_0 = \text{const}$, (7) we have:

$$S = \text{const} \cdot \ln Q. \quad (8)$$

The last expression shows the logarithmic dependence of the corrosion spot area of "defects" of the metal surface or coating. The probability of (3) can be determined, on the other hand, as the ratio of the binding energy of oxygen molecule E_0 to the metal atom to the total energy of formation of corrosion spots E . Given that [5]:

$$E_{\text{обл}} = \Delta G_T^0 = -RT 2,303 \lg K_p, \quad (9)$$

where K_p - the constant of chemical equilibrium.

For the area of corrosion spots get:

$$S = \text{const} \cdot \ln K_p \quad (10)$$

Despite the simplicity of the formulas (8) and (10), they may be useful for the study of the processes of any corrosion of structural materials, because include easily experimentally determined parameters.

2. Thermodynamic model of corrosion and mechanical failure of metals, alloys and coatings.

Considering the elementary carriers of corrosion or mechanical damage as a subsystem of non-interacting particles immersed in a thermostat, it is possible on the basis of quantum statistical thermodynamics to obtain the response function of this subsystem to the external action [13]. If the response function to take the area of corrosion spots S , we obtain:

$$S = \frac{kT}{C} \cdot \frac{A}{G^0} \cdot \bar{N} \cdot t, \quad (11)$$

where A is the work of "external forces" and T is temperature, G^0 is Gibbs potential of a bulk sample of metal - the average number of points of corrosion, t - is time of corrosion, k - is Boltzmann constant, C - is constant.

The work of "external forces" equal to the change of the standard thermodynamic potential ΔG_T , which is the basis of thermodynamics and corrosion can be determined through the chemical equilibrium constant K_p according to the formula [5]:

$$\Delta G_T^0 = -RT2,303 \lg K_p, \quad (12)$$

Corrosion starts from the surface layer and therefore in the formula (11) to make the substitution $G^0 = \sigma \cdot S_0$ - where σ - the surface tension, S_0 - specific surface. As shown in [17], the surface tension of the metal is related to its melting point ratio $\sigma = 10^{-4} \cdot T_p$.

Taking as a response function in (11) the thickness of the corrosion layer h , for corrosion rate $v_c = h/t$, which is determined experimentally, we finally obtain the following expression:

$$v_{\text{коп.}} = C_1 \frac{T^2 \lg K_p}{\sigma S} = C \cdot \frac{T^2 \lg K_p}{T_{\text{мл.}}}, \quad (13)$$

where the constant C includes all the constants of the previous formulas.

Formula (13) can be used to predict the corrosion rate of newly synthesized coating and selection of their elemental composition. For thin films and coatings surface tension value is the value of σ and additive may be determined experimentally as described in [17]. Similarly, the speed of the mechanical or thermal destruction of the coating will have the following relationships:

$$v_p = C \cdot \frac{E_F}{T_{\text{мл.}}}. \quad (14)$$

$$v_p = C_1 \cdot \frac{\mu}{\sigma}. \quad (15)$$

Equation (14) is valid for pure metals. Using the experimental values of the Fermi energy E_F , melting and corrosion rates for ten metals Au, Ag, Al, Cu, Fe, Ni, Pb, Pt, Sn, Zn, we calculated the constant C . Up to 20% of it was constant and equal to $(2,5-3,0) \cdot 10^{-4}$. Equation (15) is valid for multiple and multi-coatings. In this case, better experimentally determine the corrosion rate and the amount of tension as described in [17].

3. The corrosion resistance of components of mining equipment.

To determine the corrosion resistance of the coatings used the method of anodic polarization initiation defects (APID). For quantitative evaluation of the integral quality coatings using the integral quality parameter $K = (Q-Q_1) / Q_0$, wherein Q_0 and Q_1 - amount of electricity passed through the cell when electrical polarization uncoated surface of the sample and in the potential range covering from the start of the dissolution potential of the substrate material to the potentials on the (10-40)% less capacity starts dissolving coating material

Typically, the upper limit is selected from the interval (3-5) B. The parameter K is dimensionless and normalized. Higher quality coverage corresponds to the value $K = 1$ and $K = 0$ the lowest. The coating is applied to the following items of mining equipment: rod (steel 40X); pin 12 (steel 35); with sleeve 12 (steel 35); RU11.008-01 coupling (steel 35); cork GVU 30.002 (steel 35); gon 10NG12 (steel 35); right cheek G9.00.18 (steel 3).

However, the calculation of economic efficiency of the entire production cycle of the application of titanium nitride coatings showed that the price of the above items of mining equipment increased by approximately 20% compared to the galvanized coating applied electrolytically factory RGTO Coal Department of JSC "ArcelorMittal". It should be noted that despite the increase in the cost of coverage, galvanized coating plant RGTO obtained substandard.

Table 1 - The corrosion rate of titanium nitride coatingstechnological environment

technological environment	concentration (mass)%	temperature, °C	corrosionrate mm / year
nitricacid	80	20	0.01
sulfuricacid	52	20	0.03
hydrochloricacid	80	20	0.05

Nitriding was conducted for parts described above. Table 2 shows the comparative analysis. From Table 2 that the technology of vacuum nitriding, though inferior in corrosion resistance of titanium nitride coatings, but is much greater than the zinc coating. At the same time, the cost of nitrided parts on (10-15) % lower zinc.

In the case of small lots of parts, and also to make better use of critical parts of titanium nitride coatings which enhance corrosion resistance in addition have high strength. Vacuum nitriding is a cheaper way to increase corrosion resistance. It has distinct advantages over electrolytic zinc and chrome finish. We applied the method of ion plasma coating Fe-Al-Ti, Zn-Al-Ti, Zn-Cu-Al-Ti. Table 3 are represented by their corrosive characteristics.

Table 2 - Characteristics of various coatings

namedetails	anti-corrosioncoating	coefficient K
Coupling RU 11.008-01, steel 35	Zinc	0.15
Coupling RU 11.008-01, steel 35	Nitrated	0.40
Coupling RU 11.008-01, steel 35	Titaniumnitride	0.75

Table 3 - Characteristics of various coatings

namedetails	anti-corrosioncoating	coefficient K
Nipple 12, steel 35	Fe-Al-Ti	0,47
Coupling 12 c, steel 35	Zn-Al-Ti	0,57
CorkGVU 30,002, steel 35	Zn-Cu-Al-Ti	0,61

As can be seen from Table 3, the proposed coating are second only to the titanium nitride coating, but they are much cheaper than all the coatings shown in Table. 2. The manufacture of such cathodes without difficulty. The coating thickness is from 2 to 4 microns, so that a cathode is enough for about 12 thousand. Parts such as coupling 12 c.

4. Anti-corrosion wear-resistant coatings on parts of oilfield equipment

The problem of corrosion and protection against oil and gas and oil field equipment is becoming more urgent and acute. This is due, primarily, the increase in the number of acceding to the development of oil, gas and gas condensate (especially sea), containing corrosive components, and secondly, the increasing intensity of work of oilfield equipment under intensive production methods, transport and processing.

The high efficiency of the existing corrosion protection technology makes introduce other, more efficient technologies to reduce the corrosive wear and thereby increase the terms of use and other downhole oilfield equipment.

At present, all industrial countries are not on the path of anticorrosive steel and alloys and application technology developed by modern anti-corrosion coatings for cheaper grades of steel [18-25].

In recent years, attracted the interest of researchers high entropy alloys and coatings based on them [26-29]. In this case, the coating obtained with high performance.

This paper discusses the results of a study of the structure and properties of coatings Cr-Mn-Si-Cu-Fe-Al and Cr-Mn-Si-Cu-Fe-Al + Ti. We used methods Cr-Mn-Si-Cu-Fe-Al, produced by induction melting. The coatings were deposited by ion-plasma method on the vacuum unit HHB-6.6I1 on a sample of steel 12X18H10T. Coatings Cr-Mn-Si-Cu-Fe-Al+Ti were obtained while spraying a cathode Cr-Mn-Si-Cu-Fe-Al and a titanium cathode. Electron microscopic study was performed on a scanning electron microscope MIRA 3 firms TESCAN. Research carried out at an accelerating voltage of 20 kV and a working distance of approximately 15 mm. Each sample was done by 4 shots at 4 points on the surface at different magnifications: 245-fold, 1060-fold, 4500-fold and 14600-fold. And power dispersive analysis conducted at 4 points each specimen. The thickness of the coatings and their elemental composition is measured using an electron microscope 200 Quanta 3D. The phase composition and structural parameters of the samples was performed on diffractometer XRD-6000 X in the $\text{CuK}\alpha$ -rays. An analysis of the phase composition, the size of coherent scattering regions, the internal elastic stresses ($\Delta d/d$) carried out with use of databases PCPDFWIN and PDF4+, as well as programs POWDER CELL 2.4. For samples nanohardness coatings was determined using the method of Oliver nanoindentation system and headlamp using a Berkovich indenter with a load of 1 g and a dwell time of 15 sec. The corrosion resistance of the coatings was determined in accordance with GOST 9.908-85.

On the stainless steel substrate was coated with Cr-Mn-Si-Cu-Fe-Al in gaseous nitrogen for 40 min. Fig. 1a shows an image of the coating obtained in an atomic force microscope. Fig. 1b shows a cross section of 1 micron coating produced a focused ion beam.

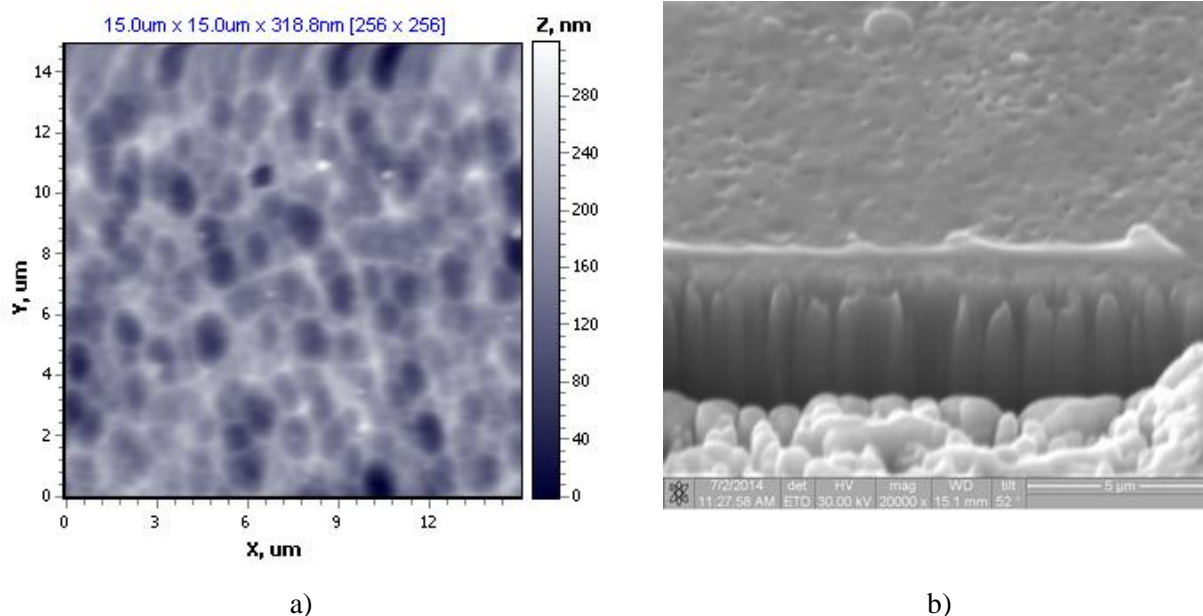


Fig.1. AFM image of the coating Cr-Mn-Si-Cu-Fe-Al (a) and cross section (b)

The results of the study of the phase composition of the sample are shown in Table 4. It was determined on the hardness of the coating Cr-Mn-Si-Cu-Fe-Al nitrogen gas, which is equal to 7.413 GPa. It was determined: modulus of flow coating which is equal to 169.5 GPa, fluidity is 0.68%, and the coating is 0.05% relaxation.

Table 4 - Phase composition of Cr-Mn-Si-Cu-Fe-Al in nitrogen gas

Coating	Phase detection	Phase content, vol. %	The lattice parameters, Å	The size of CSR, nm	$\Delta d/d \cdot 10^{-3}$
Cr-Mn-Si-Cu-Fe-Al	$\text{FeN}_{0.0324}$	60.6	$a=3.598$	103.4	3.46
	$\text{TiN}_{0.31}\text{O}_{0.31}$	39.4	$a=4.211$	25.6	5.14

To determine all the above parameters were determined by Poisson's number to coating the Cr-Mn-Si-Cu-Fe-Al nitrogen gas equal to approximately 0.30. The corrosion rate in sulfuric acid (53 wt.%) was about 0.02 mm/year. Coating structure Cr-Mn-Si-Cu-Fe-Al+Ti, while spraying the resulting composite and titanium cathodes is shown in Figure 2. It is similar to the structure of the coating Cr-Mn-Si-Cu-Fe-Al. Nanohardness coating Cr-Mn-Si-Cu-Fe-Al+Ti equal to 14.2 GPa. The corrosion rate in sulfuric acid (53 wt.%) was less than 0.01 mm/year.

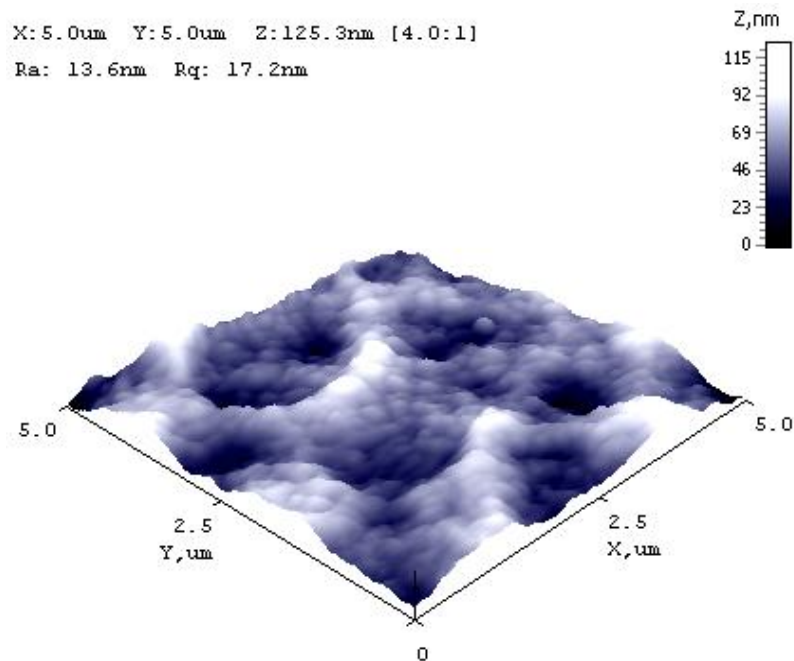


Fig.2. AFM image of the coating Cr-Mn-Si-Cu-Fe-Al+Ti under nitrogen

Figure 1b shows that the coating Cr-Mn-Si-Cu-Fe-Al is a columnar structure, which is characteristic of single-phase coatings and described by the model Thornton [30]. Single-phase structure observed in the coatings V-Zr-Nb-Hf in [31]. However, in this case there are two phases (Table 1). This suggests that the mechanism of columnar structure is not described by the model of Thornton. Below we will look at different mechanisms of such structures. It is interesting to compare the results with the known data on the nanoindentation other materials. These data are presented in Table 5.

Comparing the result obtained by us (7.413 GPa) with Table 2 shows that the nanohardness coating Cr-Mn-Si-Cu-Fe-Al almost 2 times higher nanohardness titanium and close to the Ti/ α -C:H multilayer film. However, the preparation of such a film is much more difficult than coating Cr-Mn-Si-Cu-Fe-Al composite cathode via. Nanohardness coating Cr-Mn-Si-Cu-Fe-Al+Ti (14,2GPa) is nearly amorphous ribbon nanohardness Zr-Cu-Ti-Ni (14,5 GPa) or silicon (100) (14.8 GPa). Thus, the connection between the coating reveals the structure and its hardness. For ordered structures coating hardness increases. The relationship between the hardness of the coating and its structure was discussed in [33].

Table 5 - Properties of the materials according to the calculated nanoindentation [32]

Material	H, GPa	E, GPa	R, %
Copper	2.1	121	14
Titanium	4.1	130	19
The multilayer film Ti/ α -C:H	8.0	128	34
The amorphous ribbon Zr-Cu-Ti-Ni	11.5	117	42
Silicon (100)	11.8	174	62
Thin film Ti-Si-N	28.4	295	62

5. The thermal resistance of multi-coating

Under the thermal resistance means the ability of a material to resist chemical degradation at high temperatures. Already in the 80s of the last century it became clear that you must not go towards the creation of special heat-resistant alloys and application technology to create various heat-resistant coatings on parts of machines and mechanisms operating under extreme conditions [34-36]. In subsequent years, interest in the thermally resistant materials and coatings continued to grow with the development of rocket and space technology, energy, etc. [37-39].

This paragraph is not intended to produce heat-resistant coatings. Using multi-element coverage, we would like to show the relationship between the thermal resistance and the surface energy of the coating, as well as to the method of calculating the surface energy (surface tension) of the deposited coating, using the results obtained in our work [17].

Thermal stability tests were carried out in electric furnaces resistance type G-30 in an atmosphere of air, with automatic temperature control to within $\pm 10^\circ \text{C}$. In tests we used special ceramic crucibles. The samples were placed in a crucible, which is then sent to the furnace.

Heat resistance was evaluated by weight of oxidized material. Weighing the samples before and after heat treatment was carried out on an analytical balance to the nearest 0.1 mg. Table 6 shows test results for heat resistance of the coatings.

Table 6 - The weight loss of the coating after heat treatment at 600°C for 100 hours

Coating	Oxidized coating weight, mg
Uncoated sample	56.8
Cr-Mn-Si-Cu-Fe-Al	4.2
Zn-Al	5.6
Mn-Fe-Cu-Al	6.8
Fe-Al	14.2

From Table 6 it follows that the highest thermal stability of the investigated coatings has a coating Cr-Mn-Si-Cu-Fe-Al, and the lowest - Fe-Al. However, any of the above coating greatly increases the thermal resistance substrate (metal substrate). If the response function F from [15] to take the thermal resistance χ , we obtain:

$$\chi = \frac{kT}{C_1} \cdot \frac{A}{G^0}, \quad (16)$$

where A - work of "external forces", T - temperature, the G^0 - Gibbs potential bulk metal sample (pure metal - is the Fermi energy E_F), k - Boltzmann constant, C_1 - constant.

The work of "external forces" for surface and thin films is equal to the energy of their destruction, i.e., $A = \sigma \cdot S$, where σ - surface tension, S is the specific surface. Thus, the thermal resistance is greater the greater their surface energy (surface tension). Table 7 shows the values of the investigated surface tension coatings obtained as described in [17]. Correlation between Tables 6 and 7 there.

Since $G_0 = a + bT + cT^2$, the temperature dependence of χ can be neglected and the record (16) for one-component coating in the form of:

$$\chi = C \cdot \sigma / E_F, \quad (17)$$

where C - a constant.

For a multiple-coating, when there is no separation of the individual phases, we have:

$$\chi = C \cdot \left(\sum_i X_i \cdot \sigma_i / E_{F_i} \right), \quad (18)$$

where X_i - the mole or atomic fraction of the respective element in the coating.

Table 7 - The surface tension of multi-coating

Coating	The surface tension, j/m ²
Cr-Mn-Si-Cu-Fe-Al	1.019
Zn-Al	0.594
Mn-Fe-Cu-Al	0.446
Fe-Al	0.314

Multi-element, single-phase coatings are obtained, for example, in [31]. In the case of the individual phases in the coating (nitride, sulfide, etc.), the formula (3) can not be used. In this case we can use in our work [40], where the values of surface tension for nitrides, sulfides, oxides, etc. most of the elements of the periodic table. Determination of the surface tension of solids - a difficult task, so you can use a universal relation [17]:

$$\sigma = 0,7 \cdot T_{m.m.}, \quad (19)$$

where T_m - the melting point of the metal, which is defined with great precision for all elements.

These formulas allow purposefully synthesize coating with desired thermal properties. The main problem is the generation of multi-element plasma flows. In most cases, this problem is not fundamental problems.

6. Thermomechanical destruction of metals, alloys and coatings

The destruction of the metal at the supply of thermal energy is accompanied by the accumulation of thermal stress, leading to an increase in the dislocation density, various defects (dilators, frustrons etc.) [41-44].

Most of the existing mechanical systems in nature with the free movement of scatter ordered kinetic energy of its movement and turn it into a random thermal motion of the molecules. Such systems are usually called dissipative systems. Sometimes the flow of energy supplied to the system

can reach such intensity that the old dissipation mechanism cannot cope with it. The system threatens the destruction. Then it can produce an internal reorganization of its elements in such a way that the energy dissipation process would go more intensively. This internal change occurs at phase transitions in the volume of metals and alloys [45], at the grain boundaries [46], on the surface [47]. On the basis of the theory of phase transitions attempt to combine different mechanisms of destruction processes [48]. In [49] proposes a mechanism of destruction of solids, not associated with the presence of defects in their original condition.

The theory of thermoelasticity of thin plates, and in this case coatings, as well as the corresponding isothermal theory is based on the hypothesis of the immutability of the normal element, and on the assumption of a two-dimensional stress state, a similar plane stress. The most complete questions thermoelasticity of thin plates described in [50].

In the formation of thermal stresses are distributed coating on some periodic (autowave) law [51]. Experimentally, it is shown in a periodic variation of the coating microhardness measured the length and breadth of the sample. Here we want to show the methodology for calculating the thermal stress on the experimental values of the microhardness. For this we use the heat equation for an infinite plate (cover), obtained in [52] for the radial μ_r and axial μ_z microhardness components:

$$\mu_r = A_r \frac{\partial T}{\partial r} = \frac{2}{z} \frac{A_r T_0}{\sqrt{\pi}} I_1\left(\frac{2r}{R}\right), \quad (20)$$

$$\mu_z = A_z \frac{\partial T}{\partial z} = \frac{R A_z T_0}{\sqrt{\pi z^2}} I_0\left(\frac{2r}{R}\right). \quad (21)$$

In these expressions A is a constant value with small thermal strains. The metal bodies of the effect of connectedness strain field and temperature field usually has little effect on the thermal perturbation and distribution of thermal stresses. In this case, you can use the known solutions for a circular plate of constant thickness [50]. And the stress component record:

$$\sigma_r = -2G \frac{1}{r} \frac{\partial T}{\partial r}. \quad (22)$$

$$\sigma_z = -2G \frac{\partial T}{\partial z}. \quad (23)$$

Here G is the shear modulus is given by:

$$2G = \frac{E}{1+\varepsilon}, \quad (24)$$

where E - Young's modulus, ε - Poisson's ratio.

We experimentally determined the radial component of the microhardness. Comparing (20) and (22) we obtain:

$$\sigma_r = -2G \frac{1}{r A_r} \mu_r. \quad (25)$$

Formula (25) is the basis for calculating the thermal stress in the coating on the experimental values of the microhardness.

Conclusion

Based on the analysis of the current state of destruction theories, corrosion, thermal and deformation of metals loading and coatings, as well as based on the proposed model, we can draw the following conclusions:

- in the most general case, corrosion of the metal can be present as the nucleation and growth of the new phase (oxidized metal). This is the approach used in the present study when discussing theoretical aspects of metal corrosion;
- formal description of the probabilistic nature of the new phase of the process as a random Markov stationary or non-stationary Poisson process requires a rigorous justification, as a number of assumptions (no aftereffects, ordinary, etc.) Does not stem from the physical picture of the phenomenon of corrosion;
- on the basis of a statistical approach to the formation of corrosion spots obtained an expression that shows the logarithmic dependence of the corrosion spot area of "defects" of the metal surface or coating;
- on the basis of non-equilibrium quantum statistical thermodynamics of a formula for the defects of the system response function (corrosion centers) to the external field;
- on the basis of a thermodynamic model obtained relationship between the corrosion rate, the surface tension of a metal surface and melting them;
- the theory of thermoelasticity of thin plates, and in this case coatings, as well as the corresponding isothermal theory, based on the hypothesis of the immutability of the normal element, and on the assumption of a two-dimensional stress state, a similar plane stress;
- proposed method of determining the thermal stress in the coating on the basis of experimental values of microhardness, measured the length and breadth of the sample;
- on the basis of thermodynamic model derived relationship between the heat resistance of coatings and surface energy;
- obtain a formula which is suitable for qualitative analysis and forecasting of metal fracture rate and coatings deformation and thermal influences.

REFERENCES

- 1 Strutt I.E., Nicholls and Barbier B. The prediction of corrosion by statistical analysis of corrosion profiles. *Corrosion science*. 1985, Vol. 25, No. 5, pp. 305 – 316.
- 2 Provan J.W., Rodriguez E.S. Development of a Markov description of pitting corrosion. *Corrosion (USA)*, 1989, Vol. 45, No. 3, pp. 178 – 192.
- 3 Baroux B. The kinetics of pit generation on stainless steel. *Corrosion science*, 1988, Vol. 28, No. 10, pp. 969 – 986.
- 4 Kondo J. Prediction of fatigue crack initiation life based on pit growth. *Corrosion science*, 1989, Vol. 45, No. 1, pp. 7 – 11.
- 5 Azarenkov N.A., Lytovchenko S.V., Nekludov I.M., Stoev P.I. *Corrosion and protection of metals. Part 1. Chemical corrosion of metals*. Kharkiv, 2007, 187p.
- 6 Park J.K., Baik Y.J. Increase of hardness and thermal stability of TiAlN coating by nanoscale multi-layered structurization with a BN phase. *Thin Solid Films*, 2008. Vol. 516, pp. 3661 – 3664.
- 7 Verma N., Cadambi S., Jayarama V., Biswas S.K. Micromechanisms of damage nucleation during contact deformation of columnar multilayer nitride coatings. *Acta Materialia*, 2012, Vol. 60, pp. 3063 – 3073.
- 8 Skripov V.P. *Metastable liquid*. Nauka, Moscow, 1972, 312 p.
- 9 Kidyarov B.I. *The kinetics of formation of crystals from the liquid phase*. Nauka, Novosibirsk, 1979, 134 p.
- 10 Dynkin E.B., Yushkevich A.A. *Theorems and problems on Markov processes*. Nauka, Moscow, 1967, 426 p.
- 11 Platonova E.C., Buchinskas V., Yurov V.M. Statistical model for the formation of corrosion spots on the metal. *Fundamental Research*, Russia, 2015, No.2, pp. 3048 – 3051.

- 12 Platonova E.C., Buchinskas V., Yurov V.M. Thermodynamic model of the formation of corrosion spots on the metal. *Fundamental Research*, Russia, 2015, No. 2, pp. 3281 – 3284.
- 13 Platonova E.C., Buchinskas V., Yurov V.M. Some questions of the theory of metal corrosion. *Bulletin of the University. Physics*, Kazakhstan, 2015, No.1 (77), pp. 21 – 30.
- 14 Yurov V.M., Guchenko S.A., Laurynas V.Ch. The role of the surface tension in the formation of plasma coatings. *Scientific Review. Technical science*, Russia, 2016, No. 4, pp. 124 – 139.
- 15 Platonova E.S., Zhetesova G.S., Yurov V.M., Guchenko S.A. Anticorrosion and strengthening coatings for mining equipment. *Naukova News of the National Mining University*, Ukraine, 2016, No. 2, pp. 55 – 59.
- 16 Eremin E.N., Yurov V.M., Ibatov M.K., Guchenko S.A., Laurynas V.Ch. Anti-corrosion wear-resistant coatings on parts of oil field equipment. *Procedia Engineering*, 2016, Vol. 152, pp. 594 – 600.
- 17 Yurov V.M., Laurynas V.Ch., Guchenko S.A., Zavatsky O.N. The surface tension of hardening coatings. *Reinforcing technology and coating*, Russia, 2014, No.1. – pp. 33-36.
- 18 Lopez D., Alonso Falleiros N., Tschiptschin A.P. Effect of nitrogen on the corrosion–erosion synergism in an austenitic stainless steel. *Tribology International*, 2011, Vol. 44, pp. 610–616.
- 19 Liu R., Li X., Hu X., Dong H. Surface modification of a medical grade Co-Cr-Mo alloy by low-temperature plasma surface alloying with nitrogen and carbon. *Surface and Coatings Technology*, 2013, Vol.232, pp. 906 – 911.
- 20 Lv Jinlong, Luo Hongyun. Effect of surface burnishing on texture and corrosion behavior of 2024 aluminum alloy. *Surface and Coatings Technology*, 2013, Vol. 235, pp. 513 – 520.
- 21 Lee Y.J., Lee T.H., Kim D.Y. et. al. Microstructural and corrosion characteristics of tantalum coatings prepared by molten salt electrodeposition. *Surface and Coatings Technology*, 2013, Vol. 235, pp.819 – 826.
- 22 Castillejo F.E., Marulanda D.M., Olaya J.J, Alfonso J.E. Wear and corrosion resistance of niobium–chromium carbide coatings on AISI D2 produced through TRD. *Surface and Coatings Technology*, 2014, Vol. 254, pp. 104 – 111.
- 23 Klemm J., Klemm S.O., Duarte M.J. et. al. Multi-element-resolved electrochemical corrosion analysis. Part I. Dissolution behavior and passivity of amorphous Fe₅₀Cr₁₅Mo₁₄C₁₅B₆. *Corrosion Science*, 2014, Vol. 89, pp. 59-68.
- 24 Alvarez-Asencio R., Sababi M., Pan J. et. al. Role of microstructure on corrosion initiation of an experimental tool alloy: A Quantitative Nanomechanical Property Mapping study. *Corrosion Science*, 2014, Vol. 89, pp. 236 – 241.
- 25 Skliarova H., Renzelli M., Azzolini O. et. al. Niobium–niobium oxide multilayered coatings for corrosion protection of proton-irradiated liquid water targets for [¹⁸F] production. *Thin Solid Films*, 2015, Vol. 591, pp. 316 – 322.
- 26 Otto F., Yang Y., Bei H., George E.P. Relative effects of enthalpy and entropy on the phase stability of equiatomic high-entropy alloys. *Acta Materialia*, 2013, Vol. 61, pp. 2628 – 2638.
- 27 Tsai M.H., Yeh J.W. High-entropy alloys: a critical review. *Mater. Res. Lett.*, 2014, Vol. 2, pp. 107-123.
- 28 Pogrebnyak A.D., Baghdasaryan A.A., Yakushchenko I.V., Beresnev V.M. Structure and properties of alloys and high-entropy nitride coatings on their basis. *Russian Chemical Reviews*, 2014, Vol. 83, No.11, pp. 1027 – 1061.
- 29 Schuh B., Mendez-Martin F., Vulker B. et. al. Mechanical properties, microstructure and thermal stability of a nanocrystalline Co Cr Fe Mn Ni high-entropy alloy after severe plastic deformation. *Acta Materialia*, 2015, Vol. 96, pp. 258 – 268.
- 30 Thornton J.A. Structure and topography of sputtering coatings. *Ann. Rev. Material Sci.*, 1977, Vol. 7, pp. 239 – 260.
- 31 Sabol O.V., Andreev A.A., Gorban V.F. and others. On the reproducibility of single-phase structural state multi element high entropy system Ti-V-Zr-Nb-Hf and high hard nitrides based on it as they are formed by vacuum arc method. *Technical Physics Letters*, Russia, 2012, Vol. 38, No.13, pp. 40 – 47.
- 32 Golovin Y.I. Nanoindentation and mechanical properties of solids in submicro volumes, thin surface layers and films. *Solid State Physics*, Russia, 2008, Vol. 50, No.12, pp. 2113 – 2142.

- 33 Musil J., Polakova H. Hard nanocomposite Zr-Y-N coatings, correlation between hardness and structure. *Surface and Coatings Technology*, 2000, Vol. 127, pp. 99 – 106.
- 34 Movchan B.A., Malashenko I.S. *Heat-resistant coating is deposited in a vacuum*. Kiev: Naukova Dumka, 1983, 232 p. [in Russian]
- 35 Muboyadzhyan S.A., Lesnikov V.P., Kuznetsov V.P. *Integrated protective coating of turbine blades for aircraft GTE*. Ekaterinburg: Publishing house "Kvist", 2008, 208 p.
- 36 Davis J.R. (Ed.) *Heat Resistant Materials*. ASM International, 1997, 591 p.
- 37 Reed R.C. *The Superalloys: Fundamentals and Applications*. Cambridge Univ. Press, 2006, 372p.
- 38 Gao W., Li Zh. (Eds.) *Developments in High Temperature Corrosion and Protection of Materials*. - Woodhead Publishing Ltd, 2008, 658 p.
- 39 Madhusudana Chakravarti V. *Thermal Contact Conductance*. Springer Intern. Publishing Switzerland, 2014, XVIII, 260 p.
- 40 Yurov V.M., Portnov V.S., Laurynas V.Ch. et al. *Size effects and physical properties of small particles and thin films*. Karaganda: Publ. house of the Kazakh-Russian University, 2013, 116 p.
- 41 Petrov V.A. Dilaton model of thermal fluctuations of crack. *Solid State Physics*, Russia, 1983, Vol.26, No. 11, pp. 3124 – 3127.
- 42 Zhurkov S.N. Dilaton mechanism of strength of solids. *Solid State Physics*, Russia, 1983. Vol. 25, №10 – pp. 3119-3123.
- 43 Kulikov D.V., Mekalova N.V., Zakirnichnaya M.M. *Physical nature destruction*. Ufa: UFGU, 1999, 240 p. [in Russian]
- 44 Olemskoy A.I., Katznelson A.A. *Synergetics of condensed matter*. Moscow, URSS, 2003, 336 p.
- 45 Christian J. *The theory of transformations in metals and alloys*. Moscow, Mir, 1978, 808 p.
- 46 Straumal B.B. *Phase transitions in the grain boundaries*. - Moscow, MISiS, 2004, 65 p.
- 47 Zenguil E. *Surface Physics*. Moscow, Mir, 1990, 536 p. [in Russian]
- 48 Botvina R.L. *Destruction: kinetics, mechanisms, general laws*. - M.: Nauka, 2008 – 334 p.
- 49 Panin V.E., Egorushkin V.E., Makarov M.P. et al. *Physical mesomechanics and computer construction materials*. Novosibirsk, Nauka, 1995, Vol. 1, 298 p. [in Russian]
- 50 Zarubin B.C., Kuvyrkin G.N. *Mathematical models of thermal mechanics*. Moscow, FIZMATLIT, 2002, 168 p. [in Russian]
- 51 Yurov V.M., Laurynas V.Ch., Guchenko S.A., Zavatsky O.N. Autowave processes in the formation of ion-plasma coatings. *Bulletin of the University. Physics*. Kazakhstan, 2013, No. 1 (69), pp. 56 – 66.
- 52 Yurov V.M., Laurynas V.Ch., Guchenko S.A., Zavatsky O.N. The stationary thermal field of endless metal plates nanometer thickness. *International Journal of Applied and Basic Research*, Russia, 2013, No.10, pp. 514.